HHS Public Access

Author manuscript

Kidney Int. Author manuscript; available in PMC 2018 December 01.

Published in final edited form as:

Kidney Int. 2017 December ; 92(6): 1370–1383. doi:10.1016/j.kint.2017.06.015.

Hypoxia inducible factor prolyl-4-hydroxylation in FOXD1 lineage cells is essential for normal kidney development

Hanako Kobayashi, Ph.D.[1,2], **Jiao Liu, M.S.**[3,4], **Andres A. Urrutia, Ph.D.**[1], **Mikhail Burmakin, M.D., Ph.D.**[5], **Ken Ishii, Ph.D.**[1], **Malini Rajan, Ph.D.**[1], **Olena Davidoff, M.S.**[1,2], **Zubaida Saifudeen, Ph.D.**[3,4], and **Volker H. Haase, M.D.**[1,2,6,*]

[1]Department of Medicine, Vanderbilt University School of Medicine, Nashville, Tennessee, USA

[2]Medical and Research Services, Department of Veterans Affairs Hospital, Tennessee Valley Healthcare System, Nashville, Tennessee, USA

[3]Section of Pediatric Nephrology, Department of Pediatrics, Tulane University Health Sciences Center, New Orleans, Louisiana, USA

[4]The Hypertension and Renal Centers of Excellence, Tulane University Health Sciences Center, New Orleans, Louisiana, USA

[5]Division of Vascular Biology, Department of Medical Biochemistry and Biophysics, Karolinska Institutet, Stockholm, Sweden

[6]Department of Cancer Biology and Department of Molecular Physiology and Biophysics, Vanderbilt University School of Medicine, Nashville, Tennessee, USA

Abstract

Hypoxia in the embryo is a frequent cause of intra-uterine growth retardation, low birth weight and multiple organ defects. In the kidney this can lead to low nephron endowment predisposing to chronic kidney disease and arterial hypertension. A key component in cellular adaptation to hypoxia is the hypoxia-inducible factor pathway, which is regulated by prolyl-4-hydroxylase domain (PHD) dioxygenases PHD1, PHD2 and PHD3. In the adult kidney PHD oxygen-sensors are differentially expressed in a cell type-dependent manner and control the production of erythropoietin in interstitial cells. However, the role of interstitial cell PHDs in renal development has not been examined. Here we used a genetic approach in mice to interrogate PHD function in

[*]**Correspondence:** Volker H. Haase, Department of Medicine, Division of Nephrology & Hypertension, Vanderbilt University Medical Center, C-3119A MCN, 1161 21[St] Avenue So., Nashville, Tennessee 37232-2372; volker.haase@vanderbilt.edu Tel.: 615.343.7254, Fax: 615.322.6854.

AUTHORSHIP CONTRIBUTIONS

HK and VHH conceived and designed the research studies, analyzed and interpreted data, wrote the manuscript and made the figures. HK, JL, AAU, MB, KI, MR and OL performed experiments, acquired and analyzed data. SZ provided conceptual input and helped with the interpretation of data.

DISCLOSURE

The authors declare that no conflict of interest exists. Volker H. Haase serves on the Scientific Advisory Board of Akebia Therapeutics, a company that develops prolyl-4-hydroxylase inhibitors for the treatment of anemia.

FOXD1-expressing stroma during nephrogenesis. We demonstrate that PHD2 and PHD3 are essential for normal kidney development as the combined inactivation of stromal PHD2 and PHD3 resulted in renal failure that was associated with reduced kidney size, decreased numbers of glomeruli and abnormal postnatal nephron formation. In contrast, nephrogenesis was normal in animals with individual PHD inactivation. We furthermore demonstrate that the defect in nephron formation in PHD2/PHD3 double mutants required intact hypoxia-inducible factor-2 signaling and was dependent on the extent of stromal hypoxia-inducible factor activation. Thus, hypoxia-inducible factor prolyl-4-hydroxylation in renal interstitial cells is critical for normal nephron formation.

Keywords

Hypoxia; renal development; chronic kidney disease; hypoxia-inducible factor; prolyl-4-hydroxylase; pericytes

INTRODUCTION

Hypoxia not only occurs under pathologic conditions, but also physiologically during normal development regulating stem cell behavior, cellular differentiation, proliferation and migration, as well as the reciprocal interactions between different cell types on multiple levels, thus affecting morphogenesis of the embryo and placenta. Molecular mechanisms that permit cells to adequately respond to discrepancies between oxygen demand and supply are therefore critically important for normal embryonic development. A disruption of these responses may lead to developmental abnormalities in multiple organ systems and in the worst-case scenario to intra-embryonic demise.[1]

A major and critical component of cellular hypoxia responses is the prolyl-4-hydroxylase domain (PHD) / hypoxia-inducible factor (HIF) axis, which enables cells to respond to changes in tissue oxygen levels in a rapid and controlled fashion. HIF-1 and HIF-2 are pleiotropic basic helix-loop-helix transcription factors that consist of an oxygen-sensitive α-subunit and a constitutively expressed β-subunit, also known as the aryl hydrocarbon receptor nuclear translocator ARNT, and regulate a multitude of hypoxia responses, thus allowing cells to adapt to and survive low oxygen environments.[2] Under normoxic conditions, oxygen-, iron- and 2-oxoglutarate (2OG)-dependent prolyl-4-hydroxylase domain proteins, PHD1, PHD2 and PHD3, also known as egl nine homolog (EGLN) 2, EGLN1 and EGLN3 respectively, function as oxygen sensors of this pathway. PHD enzymes initiate rapid proteasomal degradation of constitutively synthesized HIF-α subunits through hydroxylation of specific proline residues.[3] A reduction in PHD catalytic activity, for example, under hypoxic conditions or due to pharmacologic inhibition, results in HIF-α stabilization and activation of HIF transcriptional programs.[3]

Sustained discrepancies between oxygen demand and supply can result from maternal disease, utero-placental insufficiency or life at high altitude. This frequently leads to intra-uterine growth retardation (IUGR), low birth weight and increases the risk of developing diabetes, cardiopulmonary disease, stroke, arterial hypertension or chronic kidney disease (CKD) in adults.[4–6] In the developing kidney hypoxia reduces ureteric bud (UB) branching

and nephron formation[7] and results in low nephron endowment, which by itself associates with increased risk of developing CKD and/or arterial hypertension.[8, 9]

Normal kidney development is driven by multiple reciprocal and cyclical interactions between the UB and the metanephric mesenchyme (MM), which result in repeated UB branching and nephron formation.[10, 11] However, little detail is known about the role of stromal cells in this process. Renal stroma is identified by the expression of the forkhead box D1 (FOXD1) transcription factor and surrounds the cap mesenchyme (CM). FOXD1-expressing stroma plays a critical role in renal capsule development, renal progenitor differentiation and nephron formation, is important for normal vascular patterning, and ultimately gives rise to cortical and medullary interstitial fibroblast-like cells, pericytes, mesangial cells and vascular smooth muscle cells (VSMC).[12–17] As hypoxia occurs physiologically during kidney development both HIF-1α and HIF-2α have been detected in the developing kidney in a cell-type dependent manner.[18–20] Despite clear evidence of HIF pathway activation, the functional roles of cell-specific HIF signaling during renal development, however, are poorly understood and information from genetic models is limited.

In order to examine the role of interstitial HIF oxygen sensing in renal development and homeostasis, we used the Cre-loxP system to target all 3 HIF-PHDs in conjunction with HIF-1α or HIF-2α in FOXD1-expressing stromal cells. We found that mice with individual *Phd1, Phd2* or *Phd3* deletion or *Phd1/Phd2* and *Phd1/Phd3* double deletion were born with normal kidneys, whereas the combined inactivation of *Phd2* and *Phd3* resulted in abnormal kidney development, renal failure and premature death. Kidney defects in *Phd2/Phd3* double knockout mice became apparent after postnatal day (P) 7, correlated with the degree of interstitial HIF activation and were characterized by a HIF-2-dependent reduction in the number of mature nephrons and glomeruli as well as abnormal renal vasculature. Taken together, our data establish that the ability to regulate HIF prolyl-4-hydroxylation in FOXD1 stroma-derived cells is essential for normal nephron formation. Our data have implications for the therapeutic use of HIF prolyl-4-hydroxylase inhibitors, which are currently in phase 3 clinical development for renal anemia.[21]

RESULTS

Combined inactivation of Phd2 and Phd3 in FOXD1 stroma is associated with renal failure and juvenile lethality

Interstitial cells play an important role in the regulation of renal hypoxia responses. A classic example is the hypoxic induction of EPO. In order to examine the role of individual PHDs in these responses, we utilized $Foxd1^{cre/+}$ transgenic mice. In this transgenic line, the *Cre* transgene, which consists of an enhanced green fluorescent protein/Cre-recombinase (EGFP/Cre) fusion protein, is under transcriptional control of the *Foxd1* promoter (Figure 1A).[22, 23] FOXD1-expressing cells surround the CM in the nephrogenic zone, give rise to all stromal components of the developing kidney and express *Phd1, 2* and *3* (Supplemental Figure S1).

Utilizing $Foxd1^{cre/+}$ transgenic mice, we developed animals with individual or combined inactivation of PHD1, PHD2 and PHD3. Whereas $Foxd1^{cre/+}$ $Phd1^{fl/fl}$, $Foxd1^{cre/+}$ $Phd2^{fl/fl}$

and Foxd1$^{cre/+}$ *Phd3*$^{fl/fl}$ mutant mice, from hereon referred to as *Foxd1-Phd1*$^{-/-}$, *Foxd1-Phd2*$^{-/-}$ *and Foxd1-Phd3*$^{-/-}$ mutants, developed normally into adulthood, *Foxd1*$^{cre/+}$ *Phd2*$^{fl/fl}$ *Phd3*$^{fl/fl}$ double knockout mice, from hereon referred to as *Foxd1-Phd2*$^{-/-}$*-Phd3*$^{-/-}$ mutants, were small and died prematurely (Figure 1B). Differences in whole body weight between mutants and *Cre*$^{-}$ littermate controls *(Foxd1*$^{+/+}$ *Phd2*$^{fl/fl}$ *Phd3*$^{fl/fl}$*)* became statistically significant by postnatal day (P) 14 (5.0 ± 0.4 g for mutants vs. 7.3 ± 0.5 g for controls; n=8 and 12 respectively; p=0.003; Supplemental Table S1). Juvenile lethality in the mutant cohort was associated with renal failure and severe pathological changes in the kidney (Figures 1C and 1D). Kidney weight was significantly reduced in mutants compared to controls (28.2 ± 2.1 mg vs. 47.9 ± 2.5 mg in controls; n=16 and 24 respectively; p<0.0001; Supplemental Table 1), and renal defects in *Foxd1-Phd2*$^{-/-}$*-Phd3*$^{-/-}$ mutants at weaning age were characterized by tubular and vascular dilatations, tubular cyst formation, accumulation of α-smooth muscle actin (α-SMA/ACTA2)-positive interstitial and glomerular cells, glomerular sclerosis, increase in collagen matrix and *collagen type 1 alpha 1 (Col1a1)* mRNA production and increased *F4/80* mRNA levels (Figure 1E, 1F and Supplemental Figure S2). Since PHD inhibition results in normoxic HIF-α stabilization and activation of HIF signaling, we assessed the mRNA expression levels of HIF target gene *Epo*. Despite the presence of severe morphologic defects *Epo* mRNA levels in the kidney were significantly increased in 2 week-old *Foxd1-Phd2*$^{-/-}$*-Phd3*$^{-/-}$ mice, indicating that the combined deletion of *Phd2* and *Phd3* resulted in robust activation of the HIF system in FOXD1 stroma-derived interstitial cells (~80-fold increase; n=9 and 10 respectively; p<0.0001; Figure 1E). Increased *Epo* was accompanied by a small but significant increase in hematocrit (38.8% ± 1.1% vs. 35.5% ± 0.8% in controls; n=14 and 14, respectively; p<0.05).

Since HIF is known to promote angiogenesis,[24, 25] we examined the renal vasculature in *Foxd1-Phd2*$^{-/-}$*-Phd3*$^{-/-}$ kidneys. For this, we used real time PCR in conjunction with IHC to characterize the tissue expression patterns of endothelial cell marker CD31 and ACTA2. At P14 we observed significant increases in microvessel density, which correlated with elevated *Cd31* mRNA expression in whole kidney homogenates (~1.4-fold increase) (Figure 1F). Furthermore, small and medium-sized arterial vessels in *Foxd1-Phd2*$^{-/-}$*-Phd3*$^{-/-}$ kidneys were dilated and were characterized by relatively thin vessel walls (Figure 1D). Vascular changes in *Foxd1-Phd2*$^{-/-}$*-Phd3*$^{-/-}$ kidneys were associated with increased transcription of *vascular endothelial growth factor (Vegf)* in renal interstitium as demonstrated by fluorescent RNA in situ hybridization (RNA-FISH, data not shown), which is consistent with findings in adult *Foxd1-Phd2*$^{-/-}$ mice.[26] Differences in *Acta2* mRNA expression were not observed. Taken together our data demonstrate that inactivation of both PHD2 and PHD3 in stromal cells resulted in interstitial HIF activation, which led to renal failure and was associated with juvenile lethality.

Combined loss of Phd2 and Phd3 in FOXD1 stroma results in reduced nephron formation

In the mouse metanephric kidney development begins at ~ embryonic day (E) 10.5 with the formation of the UB, which induces the CM.[10, 15] Since FOXD1 stromal cells, which surround the CM, are an important source of metanephric regulatory signals and have been shown to play a critical role in the maintenance and differentiation of epithelial

progenitors,[14, 16, 17] we sought to determine at what time point during development renal defects in *Foxd1-Phd2*$^{-/-}$*-Phd3*$^{-/-}$ mice became apparent. For this we harvested kidneys from *Cre*$^{-}$ control, *Foxd1-Phd2*$^{-/-}$ and *Foxd1-Phd2*$^{-/-}$*-Phd3*$^{-/-}$ mice at P0, P7 and P14 and used routine histological methods for morphologic assessment.

Whereas *Foxd1-Phd2*$^{-/-}$ kidneys were morphologically normal and could not be distinguished from controls at either time point, kidneys from *Foxd1-Phd2*$^{-/-}$*-Phd3*$^{-/-}$ mutants were characterized by the presence of undifferentiated epithelial cells in the subcapsular cortex and a reduction in the number of differentiated proximal tubules (PT) (Figure 2). Periodic acid-Schiff (PAS) staining, which identifies polysaccharides of tubular basement and brush border membranes, demonstrated a lack of PT brush border staining in *Foxd1-Phd2*$^{-/-}$*-Phd3*$^{-/-}$ kidneys at P7 and P14 (Figure 2). In contrast, normal cortical PAS staining patterns were found in *Cre*$^{-}$ control and *Foxd1-Phd2*$^{-/-}$ kidneys at P7 indicating that nephron formation was not affected by *Phd2* inactivation.

Toluidine blue staining demonstrated that the nephrogenic zone, which consists of CM, ureteric tips (UT) and early nephron structures such as renal vesicles (RV), comma-shaped bodies (CSB) and S-shaped bodies (SSB) was morphologically similar between control, *Foxd1-Phd2*$^{-/-}$, and *Foxd1-Phd2*$^{-/-}$*-Phd3*$^{-/-}$ kidneys at P0. Differences in the size of the stromal cell compartment were not observed between control and *Foxd1-Phd2*$^{-/-}$*-Phd3*$^{-/-}$ kidneys (Supplemental Figure S3). Taken together our findings suggest that the combined inactivation of *Phd2* and *Phd3* primarily impacted the later stages of tubulogenesis, which became morphologically evident by P7 (Figure 2).

To further assess the *Foxd1-Phd2*$^{-/-}$*-Phd3*$^{-/-}$ phenotype, we performed immunohistochemistry (IHC) and analyzed nephron segment-specific gene expression in whole kidney homogenates by real time PCR. The pattern of Lotus tetragonolobus lectin (LTL) staining was consistent with a reduction in the number of mature PT (Figure 3A), which was statistically significant at P7 (156.8 ± 12.4 tubules/mm^2 for mutants vs. 300.7 ± 20.8 tubules/mm^2 for controls; n=3 each; p=0.004). Statistically significant differences were not observed at P0 (152.3 ± 15.0 tubules/mm^2 for mutants vs. 174.3 ± 14.8 tubules/mm^2 for *Cre*$^{-}$ controls; n=3 each), supporting the notion that the combined inactivation of PHD2 and PHD3 impacted postnatal nephron development, which in mice terminates within the first week after birth.[27, 28] The expression of two additional PT maturation markers, megalin and cubilin, was also significantly decreased in *Foxd1-Phd2*$^{-/-}$*-Phd3*$^{-/-}$ mutants (Supplemental Figure S4). In contrast, the staining patterns and density of Tamm-Horsfall protein (THP) / uromodulin expression, a marker for the thick ascending limb of the loop of Henle (mTAL), and lectin Dolichos biflorus agglutinin (DBA) staining, which identifies the collecting duct (CD), were comparable between control and *Foxd1-Phd2*$^{-/-}$*-Phd3*$^{-/-}$ kidneys (Figure 3B). Morphologic findings were consistent with a significant decrease in *aquaporin 1 (Aqp1)* and *sodium-phosphate co-transporter-2a (NaPi2a)* mRNA levels, whereas the mRNA expression levels of mTAL gene *Nkcc2*, which encodes the Na-K-2Cl co-transporter 2, *transient receptor potential cation channel subfamily V member 5 (Trpv5)*, which is associated with the distal tubule, and CD-specific *aquaporin 2 (Aqp2)* were not reduced. In contrast mRNA levels of *uromodulin, NaCl co-transporter (Ncc) and sodium channel epithelial 1 alpha subunit (Scnn1a)* were significantly reduced

compared to control (Figure 3C). The reduction in the number of mature nephrons in *Foxd1-Phd2*$^{-/-}$-*Phd3*$^{-/-}$ mutants was associated with a decrease in the number of glomeruli at P7 (45.0 ± 2.5 glomuruli / mm^2 in mutant vs. 58.0 ± 4.1 glomeruli / mm^2 in control; n=5 and 4, respectively; $p<0.05$; Figure 3D). In summary, our data suggest that the combined loss of PHD2 and PHD3 catalytic activity in FOXD1 stromal progenitors suppressed nephron formation, which in turn led to renal failure in juvenile mice.

SIX2-expressing progenitors are not reduced in Foxd1-Phd2$^{-/-}$-Phd3$^{-/-}$ kidneys

FOXD1 stroma-derived interstitial cells play a critical role in the maintenance and differentiation of renal epithelial progenitor cells, which are contained within the CM. The CM represents induced mesenchyme and contains several layers of cells that express multiple transcription factors, including paired box 2 (PAX2), sine oculis-related homeobox 2 (SIX2) and spalt-like transcription factor 1 (SALL1), as well as several secreted molecules.[10, 11] In order to better understand the pathogenesis of defective nephron formation in *Foxd1-Phd2*$^{-/-}$-*Phd3*$^{-/-}$ mice, we used morphologic analysis and gene expression studies to assess for potential abnormalities in the nephrogenic zones of mutant kidneys. IHC for SIX2, cytokeratin, SALL1, PAX2, neural cell adhesion molecule 1 (NCAM), E-cadherin (ECAD) and LIM homeobox protein 1 (LHX1) at E15.5 and at P0 indicated that CM volume was not reduced and that renal vesicle formation was not defective in *Foxd1-Phd2*$^{-/-}$-*Phd3*$^{-/-}$ mutants (Figure 4A and 4B). Real time PCR analysis at P0, however, demonstrated that *Six2, Sall1, and Pax2* mRNA levels in whole-kidney homogenates from *Foxd1-Phd2*$^{-/-}$-*Phd3*$^{-/-}$ mice were significantly increased compared to *Cre*$^{-}$ control (~1.8-, ~1.5- and ~1.4-fold, respectively), suggesting a moderate expansion in CM volume (Figure 4C). By P7, SIX2 expression, which is highly associated with the epithelial progenitor compartment, was no longer detectable in both control and *Foxd1-Phd2*$^{-/-}$-*Phd3*$^{-/-}$ kidneys (Figure 4A), indicating that reduced nephron formation in *Foxd1-Phd2*$^{-/-}$-*Phd3*$^{-/-}$ mutants was not associated with abnormal persistence of epithelial progenitor cells. Taken together our data suggest that *Foxd1-Phd2*$^{-/-}$-*Phd3*$^{-/-}$ mutant mice were not characterized by major defects in prenatal nephrogenesis or the diminished presence of renal progenitors.

Reduced nephron formation in Foxd1-Phd2$^{-/-}$-Phd3$^{-/-}$ kidneys is dependent on the extent of stromal HIF activation

We have previously shown in adult mice that Foxd1-Cre-mediated inactivation of PHD2 resulted in HIF-2 activation in a subset of renal interstitial cells. This was associated with increased *Epo* and *Vegf* transcription, and suggested that renal interstitial cells were heterogeneous with regard to their responsiveness to PHD2 inactivation.[26] Although HIF prolyl-4-hydroxylases regulate the activity of both HIF-1α and HIF-2α, HIF-1α was not detectable in adult *Foxd1-Phd2*$^{-/-}$ kidneys. To examine whether HIF-1α was expressed in renal stroma during development, we used IHC to investigate the cellular and spatial distribution of HIF-1α and HIF-2α in kidneys from newborn *Cre*$^{-}$ control, *Foxd1-Phd2*$^{-/-}$ and *Foxd1-Phd2*$^{-/-}$-*Phd3*$^{-/-}$ mice. In contrast to adults, nuclear HIF-1α staining was detectable in the cortex of both *Foxd1-Phd2*$^{-/-}$ and *Foxd1-Phd2*$^{-/-}$-*Phd3*$^{-/-}$ kidneys at P0 and localized predominantly to the nephrogenic zone, whereas the majority of cortical HIF-2α-expressing cells were found in the sub-nephrogenic zone, suggesting a homolog-

dependent spatial distribution pattern for HIF-α subunits in the developing cortical interstitium (Figure 5A). In the renal medulla, however, both HIF-1α- and HIF-2α-expressing interstitial cells were detected (data not shown). Consistent with the spatial distribution of HIF-2α was the distribution of *Epo* transcripts, which were not detected in the nephrogenic cortex by RNA-FISH (Figure 5B).

To determine whether abnormal nephron formation in *Foxd1-Phd2*$^{-/-}$-*Phd3*$^{-/-}$ mice correlated with the degree of interstitial HIF activation, we determined the number of HIF-1α- and HIF-2α-expressing cells in *Cre*$^{-}$ control, *Foxd1-Phd2*$^{-/-}$ and *Foxd1-Phd2*$^{-/-}$-*Phd3*$^{-/-}$ kidneys. We found that compared to *Foxd1-Phd2*$^{-/-}$ mice, the number of both HIF-1α- and HIF-2α-expressing stromal cells was significantly increased in *Foxd1-Phd2*$^{-/-}$-*Phd3*$^{-/-}$ kidneys (16.5 ± 3.3 vs. 6.5 ± 1.2 cells/0.01mm^2 for HIF-1α, and 3.32 ± 1.25 vs. 0.77 ± 0.14 cells/0.01mm^2 for HIF-2α; n = 3 and 4 and $p<0.01$ and $p<0.05$, respectively; Figure 5A). Increased presence of HIF-α expressing cells was also found in *Foxd1-von Hippel-Lindau (Vhl)*$^{-/-}$ mice, which are characterized by renal maturation defects similar to those observed in *Foxd1-Phd2*$^{-/-}$-*Phd3*$^{-/-}$ mutants (Supplemental Figure S5).

Taken together our data suggest that a) HIF-1α and HIF-2α are differentially expressed in FOXD1 stroma-derived cells during kidney development, b) that FOXD1 stroma-derived cells respond differentially to PHD2 inactivation, and c) that the development of renal maturation defects is dependent on the extent of HIF activation in renal stroma, i.e. the number of cells that express HIF-α.

Nephron formation defect in Foxd1-Phd2$^{-/-}$-Phd3$^{-/-}$ mice is dependent on HIF-2 activation

To examine to what degree HIF-1 or HIF-2 signaling contributed to defective nephron formation in *Foxd1-Phd2*$^{-/-}$-*Phd3*$^{-/-}$ mice we generated *Foxd1-Phd2*$^{-/-}$-*Phd3*$^{-/-}$-*Hif1a*$^{-/-}$ and *Foxd1-Phd2*$^{-/-}$-*Phd3*$^{-/-}$-*Hif2a*$^{-/-}$ triple mutant mice in which PHD2 and PHD3 were inactivated together with either HIF-1α or HIF-2α {recombination for all targeted 2-lox alleles was equally efficient in *Foxd1-Phd2*$^{-/-}$-*Phd3*$^{-/-}$-*Hif1a*$^{-/-}$ and *Foxd1-Phd2*$^{-/-}$-*Phd3*$^{-/-}$-*Hif2a*$^{-/-}$ mutants (Supplemental Figure S6)}. *Foxd1-Phd2*$^{-/-}$-*Phd3*$^{-/-}$-*Hif1a*$^{-/-}$ mutants developed nephron formation defects similar to those seen in *Foxd1-Phd2*$^{-/-}$-*Phd3*$^{-/-}$ mice and were characterized by small kidneys and abnormal PAS, LTL and THP staining patterns (Figure 6A and Supplemental Figure S7). Morphologic abnormalities were consistent with the reduced expression of mRNAs encoding segment-specific nephron markers (Figure 6B). Nephron formation defects in *Foxd1-Phd2*$^{-/-}$-*Phd3*$^{-/-}$-*Hif1a*$^{-/-}$ mutants were furthermore associated with enhanced ACTA2 staining in glomeruli and renal interstitium (Figure 6A). In contrast, *Foxd1-Phd2*$^{-/-}$-*Phd3*$^{-/-}$-*Hif2a*$^{-/-}$ triple mutant mice survived to adulthood, had normal-sized kidneys and did not display any developmental defects or differences in the expression of mRNAs encoding epithelial or vascular markers compared to *Cre*$^{-}$ littermate controls. However, *Epo* mRNA levels were severely reduced in *Foxd1-Phd2*$^{-/-}$-*Phd3*$^{-/-}$-*Hif2a*$^{-/-}$ kidneys, which is an expected finding as renal *Epo* transcription is HIF-2-dependent (Figure 6B).[29] Foxd1-Cre-mediated deletion of *Hif1a* or *Hif2a* alone did not result in renal maturation defects although smaller body and kidney weight were observed in *Foxd1-Hif1a*$^{-/-}$ mice at P14 (Supplemental Figure S8). Our data

demonstrate that inactivation of HIF-2α but not HIF-1α in FOXD1 stroma was sufficient to restore normal nephron formation in *Foxd1-Phd2*$^{-/-}$*-Phd3*$^{-/-}$ mutant mice.

DISCUSSION

Here we have developed several genetic models to investigate the role of individual HIF prolyl-4-hydroxylases in renal homeostasis. We demonstrate that the HIF oxygen-sensing pathway in FOXD1 stroma has a crucial function during nephrogenesis and that the ability to hydroxylate HIF-2α via PHD2 and PHD3 is required for normal nephron formation. Our data suggest that PHD2 is indispensable for normal physiologic control of interstitial HIF activity during renal development, as it functions as the main HIF prolyl-4-hydroxylase in FOXD1 stroma-derived interstitial cells, whereas PHD3 is dispensable in the presence of PHD2, but becomes rate-limiting when PHD2 catalytic activity is inhibited or absent (Figure 7). We furthermore provide evidence for a distinct and non-overlapping spatial distribution of interstitial HIF-1α and HIF-2α during development and propose that physiologic control of HIF-2 signaling in renal stroma is critically important for normal kidney development.

Experimental intrauterine hypoxia has been shown to affect kidney development and postnatal renal function at multiple levels and is associated with low kidney weight at birth, low nephron endowment, reduced glomerular number and abnormal intrarenal vascular regulation.[7, 30–33] Our genetic studies establish that the stromal PHD/HIF axis is a critical component of the renal hypoxia response system that regulates late nephrogenesis in a HIF-2-dependent manner. However, the developmental impact of HIF activation and the role of individual HIF transcription factors in other cell types is less clear. Whereas mice with germline HIF-1α deletion die in utero between E9.5 and E11 precluding studies of renal development,[34, 35] hypoxia and wide-spread induction of HIF-1 signaling has been shown to restrict branching morphogenesis *in vitro*, possibly through the release of anti-branching factors.[33] Genetic HIF activation in UB cells specifically increased kidney size and number of glomeruli and very modestly enhanced UB branching, whereas UB-directed HIF-1α inactivation had the opposite effect, suggesting cell type-dependent functions of renal HIF signaling during development.[33] In contrast renal development was reported to be normal in a mixed-background strain of mice with germ line HIF-2α inactivation.[20] Normal kidney development was also reported in a genetic model of renal epithelial HIF activation generated by *Vhl* gene deletion in SIX2^{+} epithelial progenitor cells.[36] *Six2-Cre-Vhl* mutant mice, however, developed renal failure as adults. Whether nephron endowment was affected in this model is unclear. Furthermore, defects in renal development were not reported in endothelial cell-specific HIF knockout models.[37] These studies, together with our data, support the concept of cell type-dependent roles of individual HIF transcription factors in renal organogenesis.

Our studies have implications for human biology that reach beyond gestational hypoxia as PHD inhibitors are currently clinical development for renal anemia.[38] Some of the inhibiting compounds display preferential activity for certain PHDs, to what degree individual compounds have negative impact on nephrogenesis will have to be examined.[21]

Although the *Foxd1-Phd2*$^{-/-}$*-Phd3*$^{-/-}$ mutant phenotype is complex and involves multiple cell types, our studies indicate that it is dependent on the extent on stromal HIF activation, i.e. the number/density of HIF-α-expressing cells in the kidney (Figure 7). Although PHD2 is the main regulator of HIF in many cell types, PHD1 and PHD3 dioxygenases play a significant role in controlling HIF activity in a context and cell type-dependent manner.[3, 39–41] Our genetic data establish that PHD2 catalysis alone is sufficient for HIF-α degradation in FOXD1 stroma-derived interstitial cells, as the individual or combined inactivation of *Phd1* and *Phd3* alone does not result in detectable HIF-α stabilization. We also establish that PHD3, but not PHD1 (data not shown), is capable of suppressing HIF-α stabilization in a large subpopulation of *Phd2*$^{-/-}$ interstitial cells, as *Foxd1-Phd2*$^{-/-}$*-Phd3*$^{-/-}$ mutants were characterized by a significant increase in the number of stromal cells with stabilized HIF-α compared to *Foxd1-Phd2*$^{-/-}$ mutants. Differential sensitivity of renal stroma to genetic *Phd2* deletion may be due to differences in PHD3 expression levels as previously suggested,[26] which may indicate that renal interstitial cells display differential responsiveness to hypoxia.[39, 41]

In summary, our genetic studies establish a critical role for stromal HIF oxygen sensing in nephrogenesis. Our findings provide strong rationale for further investigations into oxygen-regulated signals that control intercellular crosstalk during renal development and have implications for clinical studies that investigate the therapeutic potential of PHD inhibitors in humans.

METHODS AND MATERIALS

Generation and genotyping of mice and animal procedures

The generation and genotyping of mice with floxed alleles for *Phd1 (Egln2), Phd2 (Egln1)*, and *Phd3 (Egln3), Hif1a*, and *Hif2a (Epas1)* has been described elsewhere.[42–44] *Foxd1-Phd2*$^{-/-}$*-Phd3*$^{-/-}$ were generated by breeding *Foxd1*$^{cre/+}$ *Phd2*$^{fl/+}$ *Phd3*$^{fl/fl}$ mice with Cre-negative *Foxd1*$^{+/+}$ *Phd2*$^{fl/fl}$ *Phd3*$^{fl/fl}$ homozygous mice. Only *Cre*$^{-}$ littermates served as controls. Details regarding animal work can be found in Supplemental Methods and Materials.

RNA analysis and immunohistochemistry

Technical details can be found in Supplemental Methods and Materials.

Statistics

Data are reported as mean ± SEM. Statistical analysis were performed with Prism 6 software (GraphPad Software Inc.) using Student's *t* test or 1-way ANOVA with Tukey's post hoc analysis. The survival curve was analyzed using the Kaplan-Meier method and groups were compared by log-rank test. P-values of less than 0.05 were considered statistically significant. *Study approval and ethical permits.* All procedures involving mice were performed in accordance with NIH guidelines for the use and for care of live animals and were approved by the Vanderbilt University Institutional Animal Care and Use Committee.

Supplementary Material

Refer to Web version on PubMed Central for supplementary material.

Acknowledgments

VHH is supported by the Krick-Brooks chair in Nephrology, NIH grants R01-DK101791 and R01-DK081646, and a Department of Veterans Affairs Merit Award (1I01BX002348). Additional support was provided by Vanderbilt's Diabetes Research and Training Center (P30-DK20593). The authors wish to thank Peter Ratcliffe and Tammie Bishop, University of Oxford, for generously providing the PM8 HIF2α antibody. Whole slide imaging was performed in the Digital Histology Shared Resource at Vanderbilt University Medical Center.

References

1. Dunwoodie SL. The role of hypoxia in development of the Mammalian embryo. Dev Cell. 2009; 17:755–773. [PubMed: 20059947]
2. Semenza GL. Oxygen sensing, hypoxia-inducible factors, and disease pathophysiology. Annu Rev Pathol. 2014; 9:47–71. [PubMed: 23937437]
3. Kaelin WG Jr, Ratcliffe PJ. Oxygen sensing by metazoans: the central role of the HIF hydroxylase pathway. Mol Cell. 2008; 30:393–402. [PubMed: 18498744]
4. Marsal K. Intrauterine growth restriction. Curr Opin Obstet Gynecol. 2002; 14:127–135. [PubMed: 11914689]
5. Rueda-Clausen CF, Morton JS, Davidge ST. Effects of hypoxia-induced intrauterine growth restriction on cardiopulmonary structure and function during adulthood. Cardiovasc Res. 2009; 81:713–722. [PubMed: 19088083]
6. Moore LG, Charles SM, Julian CG. Humans at high altitude: hypoxia and fetal growth. Respir Physiol Neurobiol. 2011; 178:181–190. [PubMed: 21536153]
7. Wilkinson LJ, Neal CS, Singh RR, et al. Renal developmental defects resulting from in utero hypoxia are associated with suppression of ureteric beta-catenin signaling. Kidney Int. 2015; 87:975–983. [PubMed: 25587709]
8. Keller G, Zimmer G, Mall G, et al. Nephron number in patients with primary hypertension. N Engl J Med. 2003; 348:101–108. [PubMed: 12519920]
9. Hoy WE, Hughson MD, Bertram JF, et al. Nephron number, hypertension, renal disease, and renal failure. J Am Soc Nephrol. 2005; 16:2557–2564. [PubMed: 16049069]
10. Little MH, McMahon AP. Mammalian kidney development: principles, progress, and projections. Cold Spring Harb Perspect Biol. 2012; 4
11. Krause M, Rak-Raszewska A, Pietila I, et al. Signaling during Kidney Development. Cells. 2015; 4:112–132. [PubMed: 25867084]
12. Hatini V, Huh SO, Herzlinger D, et al. Essential role of stromal mesenchyme in kidney morphogenesis revealed by targeted disruption of Winged Helix transcription factor BF-2. Genes Dev. 1996; 10:1467–1478. [PubMed: 8666231]
13. Levinson RS, Batourina E, Choi C, et al. Foxd1-dependent signals control cellularity in the renal capsule, a structure required for normal renal development. Development. 2005; 132:529–539. [PubMed: 15634693]
14. Das A, Tanigawa S, Karner CM, et al. Stromal-epithelial crosstalk regulates kidney progenitor cell differentiation. Nat Cell Biol. 2013; 15:1035–1044. [PubMed: 23974041]
15. Gomez IG, Duffield JS. The FOXD1 lineage of kidney perivascular cells and myofibroblasts: functions and responses to injury. Kidney Int Suppl (2011). 2014; 4:26–33. [PubMed: 26312147]
16. Fetting JL, Guay JA, Karolak MJ, et al. FOXD1 promotes nephron progenitor differentiation by repressing decorin in the embryonic kidney. Development. 2014; 141:17–27. [PubMed: 24284212]
17. Nakagawa N, Xin C, Roach AM, et al. Dicer1 activity in the stromal compartment regulates nephron differentiation and vascular patterning during mammalian kidney organogenesis. Kidney Int. 2015; 87:1125–1140. [PubMed: 25651362]

18. Freeburg PB, Robert B, St John PL, et al. Podocyte expression of hypoxia-inducible factor (HIF)-1 and HIF-2 during glomerular development. J Am Soc Nephrol. 2003; 14:927–938. [PubMed: 12660327]
19. Bernhardt WM, Schmitt R, Rosenberger C, et al. Expression of hypoxia-inducible transcription factors in developing human and rat kidneys. Kidney Int. 2006; 69:114–122. [PubMed: 16374431]
20. Steenhard BM, Freeburg PB, Isom K, et al. Kidney development and gene expression in the HIF2alpha knockout mouse. Dev Dyn. 2007; 236:1115–1125. [PubMed: 17342756]
21. Haase VH. HIF-prolyl hydroxylases as therapeutic targets in erythropoiesis and iron metabolism. Hemodial Int. 2017; 21(Suppl 1):S110–S124. [PubMed: 28449418]
22. Humphreys BD, Lin SL, Kobayashi A, et al. Fate tracing reveals the pericyte and not epithelial origin of myofibroblasts in kidney fibrosis. Am J Pathol. 2010; 176:85–97. [PubMed: 20008127]
23. Kobayashi A, Mugford JW, Krautzberger AM, et al. Identification of a multipotent self-renewing stromal progenitor population during mammalian kidney organogenesis. Stem Cell Reports. 2014; 3:650–662. [PubMed: 25358792]
24. Bertout JA, Patel SA, Simon MC. The impact of O2 availability on human cancer. Nat Rev Cancer. 2008; 8:967–975. [PubMed: 18987634]
25. Carmeliet P, Jain RK. Molecular mechanisms and clinical applications of angiogenesis. Nature. 2011; 473:298–307. [PubMed: 21593862]
26. Kobayashi H, Liu Q, Binns TC, et al. Distinct subpopulations of FOXD1 stroma-derived cells regulate renal erythropoietin. J Clin Invest. 2016; 126:1926–1938. [PubMed: 27088801]
27. Hartman HA, Lai HL, Patterson LT. Cessation of renal morphogenesis in mice. Dev Biol. 2007; 310:379–387. [PubMed: 17826763]
28. Rumballe BA, Georgas KM, Combes AN, et al. Nephron formation adopts a novel spatial topology at cessation of nephrogenesis. Dev Biol. 2011; 360:110–122. [PubMed: 21963425]
29. Kapitsinou PP, Liu Q, Unger TL, et al. Hepatic HIF-2 regulates erythropoietic responses to hypoxia in renal anemia. Blood. 2010; 116:3039–3048. [PubMed: 20628150]
30. Figueroa H, Lozano M, Suazo C, et al. Intrauterine growth restriction modifies the normal gene expression in kidney from rabbit fetuses. Early Hum Dev. 2012; 88:899–904. [PubMed: 22944138]
31. Tang J, Zhu Z, Xia S, et al. Chronic hypoxia in pregnancy affected vascular tone of renal interlobar arteries in the offspring. Sci Rep. 2015; 5:9723. [PubMed: 25983078]
32. Gonzalez-Rodriguez P Jr, Tong W, Xue Q, et al. Fetal hypoxia results in programming of aberrant angiotensin ii receptor expression patterns and kidney development. Int J Med Sci. 2013; 10:532–538. [PubMed: 23532764]
33. Schley G, Scholz H, Kraus A, et al. Hypoxia inhibits nephrogenesis through paracrine Vegfa despite the ability to enhance tubulogenesis. Kidney Int. 2015; 88:1283–1292. [PubMed: 26200943]
34. Iyer NV, Kotch LE, Agani F, et al. Cellular and developmental control of O2 homeostasis by hypoxia-inducible factor 1 alpha. Genes Dev. 1998; 12:149–162. [PubMed: 9436976]
35. Ryan HE, Lo J, Johnson RS. HIF-1 alpha is required for solid tumor formation and embryonic vascularization. EMBO J. 1998; 17:3005–3015. [PubMed: 9606183]
36. Wang SS, Gu YF, Wolff N, et al. Bap1 is essential for kidney function and cooperates with Vhl in renal tumorigenesis. Proc Natl Acad Sci U S A. 2014; 111:16538–16543. [PubMed: 25359211]
37. Kapitsinou PP, Sano H, Michael M, et al. Endothelial HIF-2 mediates protection and recovery from ischemic kidney injury. J Clin Invest. 2014; 124:2396–2409. [PubMed: 24789906]
38. Koury MJ, Haase VH. Anaemia in kidney disease: harnessing hypoxia responses for therapy. Nat Rev Nephrol. 2015; 11:394–410. [PubMed: 26055355]
39. Appelhoff RJ, Tian YM, Raval RR, et al. Differential function of the prolyl hydroxylases PHD1, PHD2, and PHD3 in the regulation of hypoxia-inducible factor. J Biol Chem. 2004; 279:38458–38465. [PubMed: 15247232]
40. Berra E, Benizri E, Ginouves A, et al. HIF prolyl-hydroxylase 2 is the key oxygen sensor setting low steady-state levels of HIF-1alpha in normoxia. EMBO J. 2003; 22:4082–4090. [PubMed: 12912907]

41. Minamishima YA, Moslehi J, Padera RF, et al. A feedback loop involving the Phd3 prolyl hydroxylase tunes the mammalian hypoxic response in vivo. Mol Cell Biol. 2009; 29:5729–5741. [PubMed: 19720742]

42. Takeda K, Ho VC, Takeda H, et al. Placental but not heart defects are associated with elevated hypoxia-inducible factor alpha levels in mice lacking prolyl hydroxylase domain protein 2. Mol Cell Biol. 2006; 26:8336–8346. [PubMed: 16966370]

43. Gruber M, Hu CJ, Johnson RS, et al. Acute postnatal ablation of Hif-2alpha results in anemia. Proc Natl Acad Sci U S A. 2007; 104:2301–2306. [PubMed: 17284606]

44. Ryan HE, Poloni M, McNulty W, et al. Hypoxia-inducible factor-1alpha is a positive factor in solid tumor growth. Cancer Res. 2000; 60:4010–4015. [PubMed: 10945599]

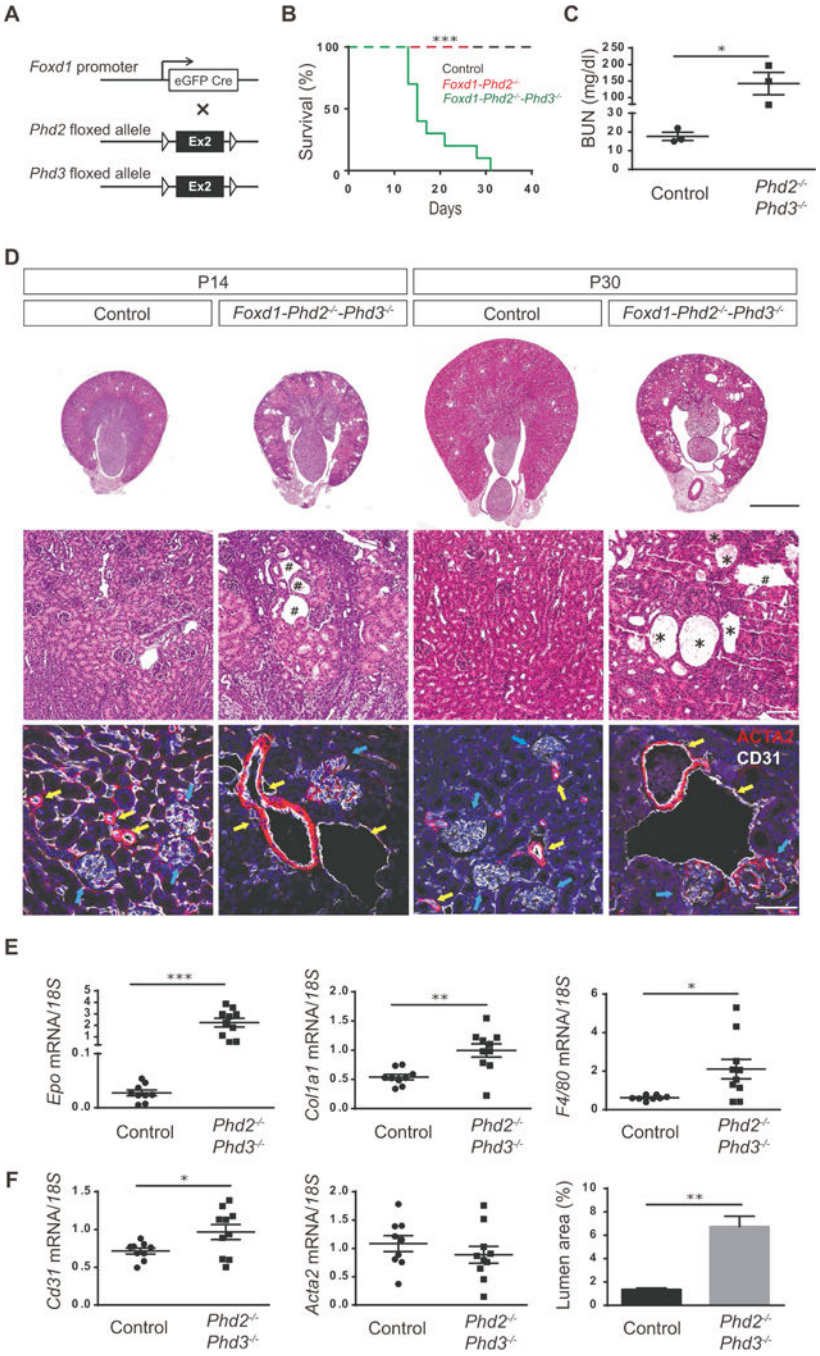

Figure 1. Combined inactivation of *Phd2* and *Phd3* in FOXD1 stroma results in renal failure

(A) Schematic illustrating the experimental approach and location of targeted sequences within the *Phd2* and *Phd3* floxed alleles. (B) Survival curve of *Cre*$^{-}$ littermate controls (*Foxd1*$^{+/+}$ *Phd2*$^{fl/fl}$ and *Foxd1*$^{+/+}$ *Phd2*$^{fl/fl}$ *Phd3*$^{fl/fl}$ mice), *Foxd1-Phd2*$^{-/-}$ and *Foxd1-Phd2*$^{-/-}$*-Phd3*$^{-/-}$ mice. Kaplan-Meier curves were plotted and compared using the log-rank test (n>10), ***p<0.001. (C) Blood urea nitrogen (BUN) from *Cre*$^{-}$ littermate control and *Foxd1-Phd2*$^{-/-}$*-Phd3*$^{-/-}$ mice at P14–P17 (n=3 each). (D) Shown are representative H&E images and immunostaining for ACTA2 and CD31 of kidney sections from *Cre*$^{-}$ control and

Foxd1-Phd2$^{-/-}$*Phd3*$^{-/-}$ mice at P14 and P30. Asterisks depict cysts, # depicts dilated vessels, yellow arrows indicate vascular walls, and blue arrows indicate glomeruli. Scale bars represent 1 mm for whole kidney cross-sections, 100 μm for high-power H&E images, and 50 μm for ACTA2/CD31 immunostaining. (E and F) *Epo, collagen type 1 alpha 1 (Col1a1)*, and *F4/80* mRNA levels in *Cre*$^{-}$ littermate control and *Foxd1-Phd2*$^{-/-}$*-Phd3*$^{-/-}$ mutant kidneys at P14 (n=8–10). Vascular lumina were quantified and are represented as total lumen area per tissue area (n=3 each). Data are represented as mean ± SEM; 2-tailed Student's *t*-test; *p<0.05, **p<0.01 and ***p<0.001.

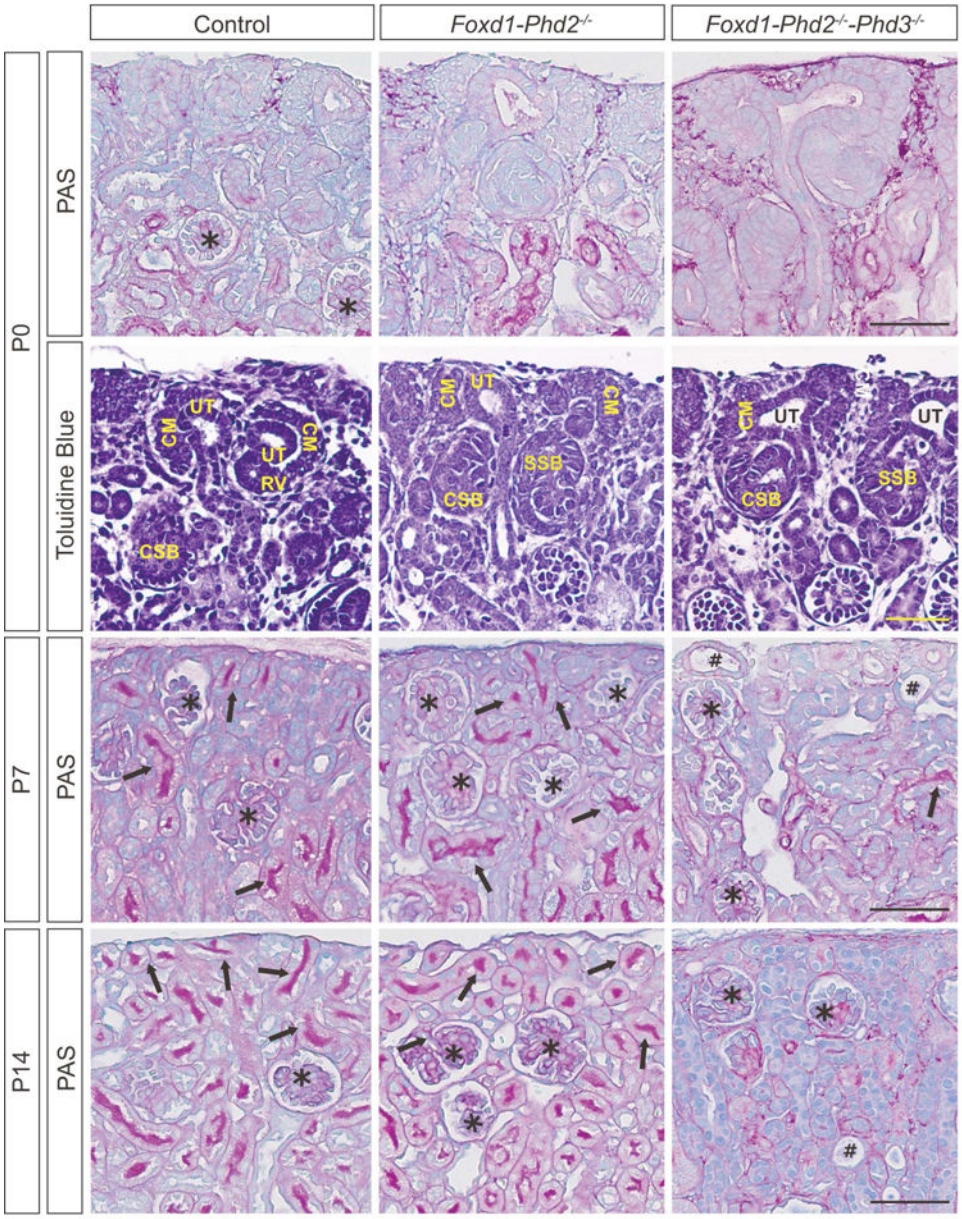

Figure 2. Defective nephron formation in *Foxd1-Phd2*$^{-/-}$-*Phd3*$^{-/-}$ mice

Shown are representative images of Periodic acid-Schiff (PAS)-stained kidney sections from *Cre*$^{-}$ control (*Foxd1*$^{+/+}$ *Phd2*$^{fl/fl}$ *Phd3*$^{fl/fl}$ for P0, and *Foxd1*$^{+/+}$ *Phd2*$^{fl/fl}$ for P7 and P14), *Foxd1-Phd2*$^{-/-}$ and *Foxd1-Phd2*$^{-/-}$-*Phd3*$^{-/-}$ mice at P0, P7 and P14, and toluidine blue-stained kidney sections from P0 animals. Arrows indicate PAS-positive mature tubules, asterisks depict glomeruli, and # marks dilated tubules. Scale bar represents 50 μm.

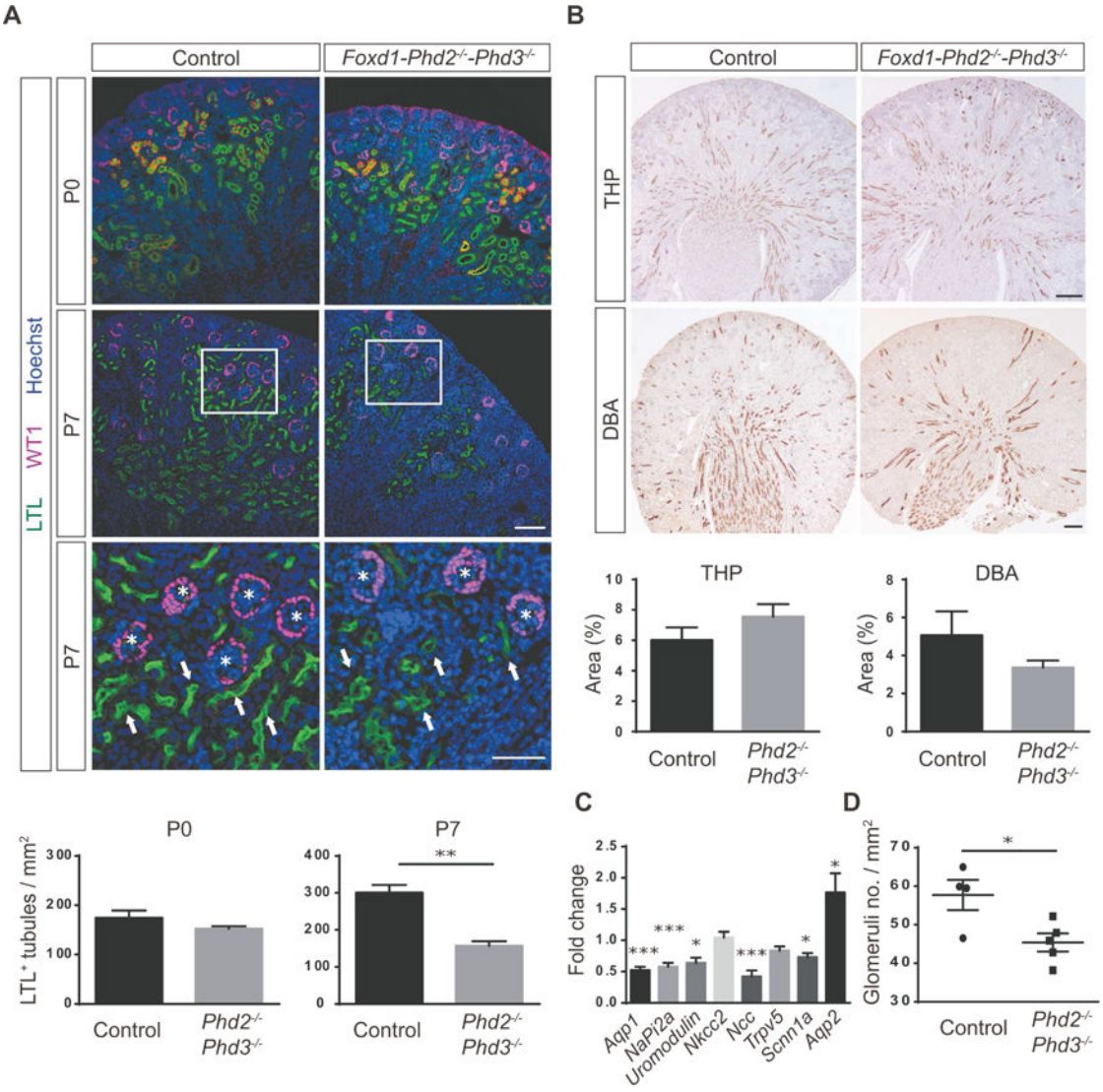

Figure 3. Combined inactivation of *Phd2* and *Phd3* in FOXD1 stroma reduces nephron formation

(A) Shown are representative images of Lotus tetragonolobus lectin (LTL) staining (green) and IHC staining for Wilms tumor 1 (WT1) (pink); kidney sections were obtained from *Cre*$^{-}$ littermate control or *Foxd1-Phd2*$^{-/-}$*-Phd3*$^{-/-}$ mutants at P0 or P7. Nuclei were stained with Hoechst dye. Arrows indicate proximal tubules and asterisks depict glomeruli. Scale bars: 100 μm (top and middle panels) and 50 μm (bottom panel). LTL^{+} tubules were quantified (n=3 each) for P0 and P7. (B) Shown are representative images of IHC staining for Tamm-Horsfall protein (THP) and Dolichos biflorus agglutinin (DBA) lectin staining of kidney sections from *Cre*$^{-}$ littermate controls and *Foxd1-Phd2*$^{-/-}$*-Phd3*$^{-/-}$ mice at P7. THP^{+} and DBA^{+} tubules were quantified (n=3–5). Scale bar: 200 μm. (C) Fold changes in mRNA expression levels of nephron segment-specific genes in total kidney homogenates *fromFoxd1-Phd2*$^{-/-}$*-Phd3*$^{-/-}$ mutants compared to *Cre*$^{-}$ littermate controls (n=8 each). (D) Quantification of glomerular numbers. Shown are number of glomeruli per mm^{2} (n=4–5). Data are represented as mean ± SEM; 2-tailed Student's *t*-test, *p<0.05, **p<0.01 and ***p<0.001. *Acta 2, α-smooth muscle actin; Aqp1, aquaporin 1; Aqp2, aquaporin 2;*

NaPi2a, sodium-phosphate co-transporter-2a; Ncc NaCl co-transporter; Nkcc2, Na-K-2Cl co-transporter, Scnn1a, sodium channel epithelial 1 alpha subunit; Trpv5, transient receptor potential cation channel subfamily V member 5.

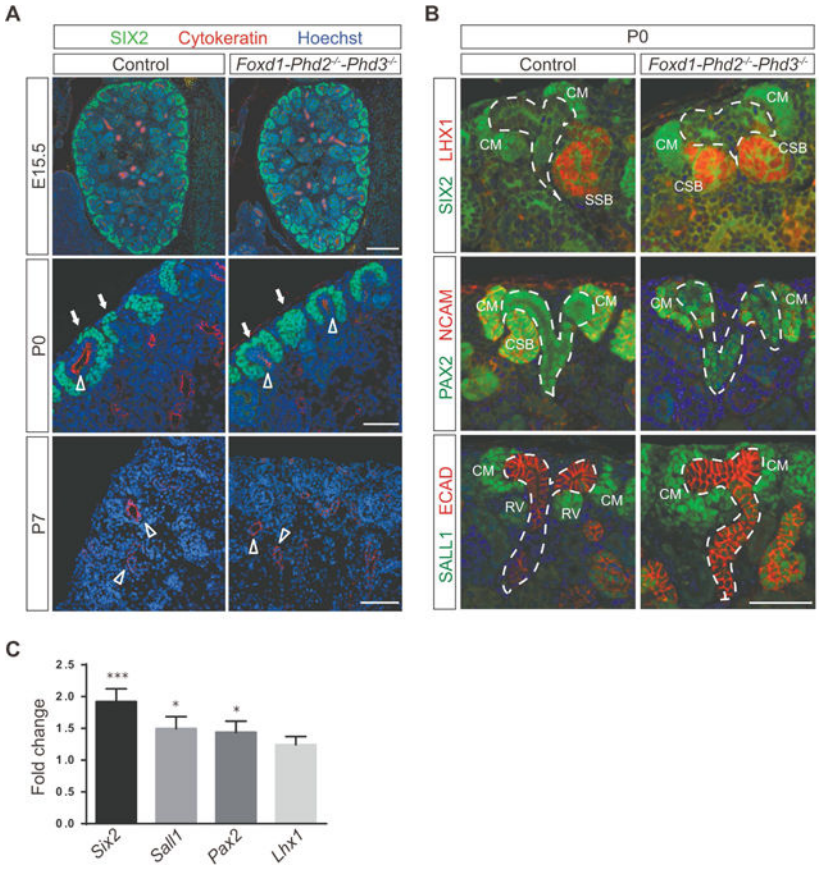

Figure 4. Nephron progenitors are not decreased in *Foxd1-Phd2*$^{-/-}$*-Phd3*$^{-/-}$ kidneys

(A) Representative images of IHC staining of formalin-fixed paraffin-embedded kidney sections for nephron progenitor marker SIX2 (green) and UB marker pan-cytokeratin (red); shown are results for *Cre*$^{-}$ littermate control and *Foxd1-Phd2*$^{-/-}$*-Phd3*$^{-/-}$ mutants at embryonic day (E) 15.5, P0 or P7. Nuclei were stained with Hoechst dye. Scale bar: 200 μm (E15.5) and 50 μm (P0 and P7). Arrows indicate cap mesenchyme and open arrowheads depict ureteric bud. (B) Shown are representative images of SIX2 (green) and LXH1 (red) (top panels), PAX2 (green) and NCAM (red) (middle panels), and SALL1 (green) and ECAD (red) (bottom panels) IHC staining of formalin-fixed paraffin-embedded kidney sections from *Cre*$^{-}$ littermate control and *Foxd1-Phd2*$^{-/-}$*-Phd3*$^{-/-}$ mice at P0. Nuclei were stained with Hoechst dye. Ureteric trees are outlined by dashed white lines and cap mesenchyme (CM), renal vesicle (RV), comma shaped body (CSB), and S-shaped body (CSB) are annotated. Scale bar: 50 μm. (C) Fold changes in *Six2, Sall1, Pax2* and *Lhx1* mRNA expression levels in total kidney homogenates from *Foxd1-Phd2*$^{-/-}$*-Phd3*$^{-/-}$ at P0 compared to *Cre*$^{-}$ littermate controls (n=12 for control and n=10 for mutants). Data are represented as mean ± SEM; 2-tailed Student's *t*-test; ***p<0.001 and *p<0.05.

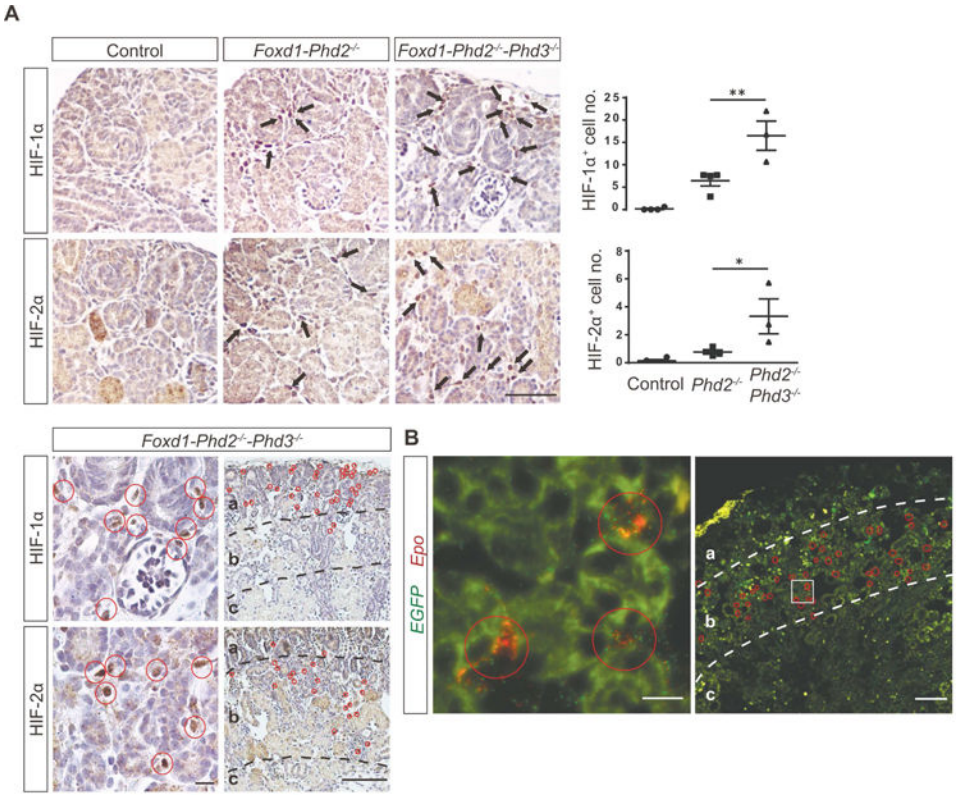

Figure 5. *Phd3* inactivation in *Phd2*$^{-/-}$ FOXD1 stroma increases the number of HIF-α expressing cells

(A) Shown are representative images of HIF-1α and HIF-2α IHC staining of formalin-fixed, paraffin-embedded kidney sections from *Cre*$^{-}$ control *(Foxd1*$^{+/+}$ *Phd2*$^{fl/fl}$ *and Foxd1*$^{+/+}$ *Phd2*$^{fl/fl}$ *Phd3*$^{fl/fl}$*), Foxd1-Phd2*$^{-/-}$ and *Foxd1-Phd2*$^{-/-}$*-Phd3*$^{-/-}$ mice at P0 (n=3–4). Arrows depict HIF-α^{+} cells. To facilitate visualization and to provide an overview of HIF-α^{+} cell distribution at low magnification, HIF-α^{+} cells were annotated with red circles (bottom right panels). The extent of stromal HIF activation is expressed as HIF-α^{+} cell number per 0.01 mm^{2}. The *Cre*$^{-}$ control group consisted of one *Foxd1*$^{+/+}$ *Phd2*$^{fl/fl}$ and three *Foxd1*$^{+/+}$ *Phd2*$^{fl/fl}$ *Phd3*$^{fl/fl}$ mice. Data represent mean ± SEM and were analyzed by 1-way ANOVA; **p<0.01. Scale bar: 50 μm (top panels), 10 μm (high-magnification images, bottom left panels), and 100 μm (low-magnification images, bottom, right panels). (B) Shown are images illustrating the distribution of *Epo*$^{+}$ cells in *Foxd1-mJ/mG-Phd2*$^{-/-}$*-Phd3*$^{-/-}$ kidneys by RNA-FISH. To facilitate visualization and to provide an overview of *Epo*$^{+}$ cell distribution at low magnification, *Epo*$^{+}$ cells were annotated with red circles (right panel). *Epo* transcripts were detected by red fluorescence and *EGFP* transcripts (cells with a history of *Foxd1-cre* expression) were detected by green fluorescence (left panel). Scale bars: 10 μm (left) and 100 μm (right). Labeling of low-magnification images in (A) and (B): (a), superficial cortex with nephrogenic zone; (b), deeper cortex and(c), medulla.

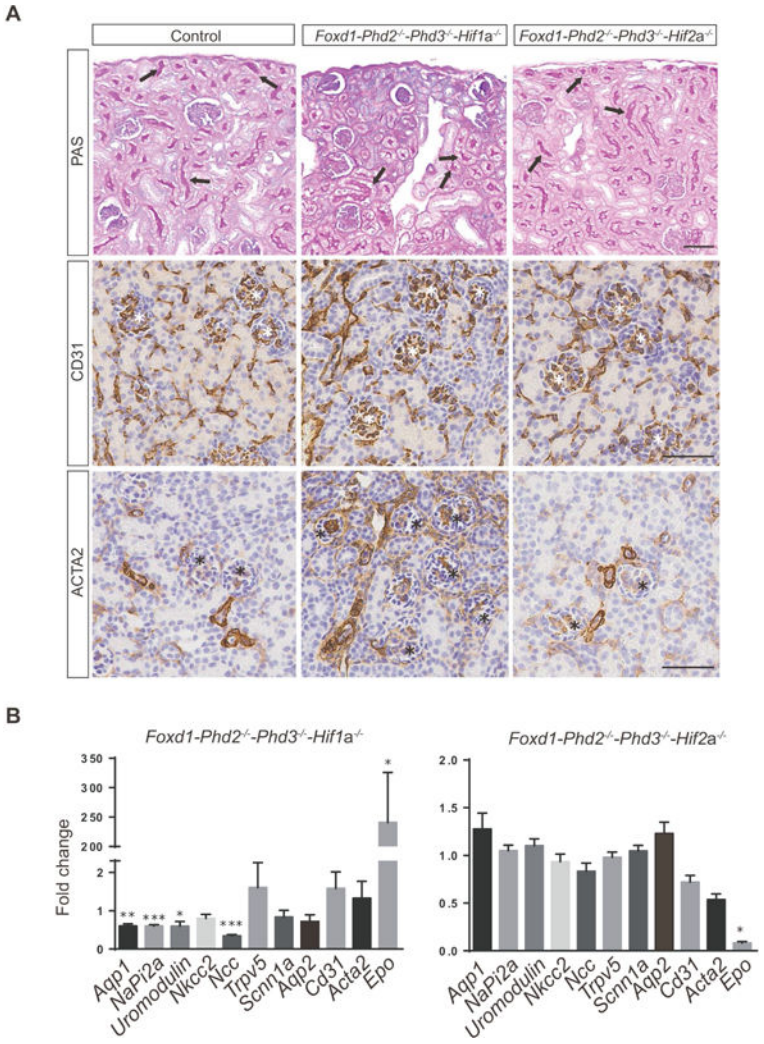

Figure 6. Nephron formation defects in *Foxd1-Phd2*$^{-/-}$-*Phd3*$^{-/-}$ mice require HIF-2α.

(A) Shown are representative images of Periodic acid-Schiff (PAS)-stained kidney sections (top) and CD31-and ACTA2 IHC staining (middle and lower panels) for *Cre*$^{-}$ control *(Foxd1*$^{+/+}$ *Phd2*$^{fl/fl}$ *Phd3*$^{fl/fl}$ *Hif2a*$^{fl/fl}$*), Foxd1-Phd2*$^{-/-}$*-Phd3*$^{-/-}$*-Hif1a*$^{-/-}$ and *Foxd1-Phd2*$^{-/-}$*-Phd3*$^{-/-}$*-Hif2a*$^{-/-}$ mutant kidneys at P14. Asterisks depict glomeruli and arrows indicate renal tubules with PAS-positive brush borders. Scale bars represent 50μm. (B) mRNA expression levels of *Epo*, nephron-segment-specific and vascular markers in whole kidney homogenates from *Foxd1-Phd2*$^{-/-}$*-Phd3*$^{-/-}$*-Hif1a*$^{-/-}$ and *Foxd1-Phd2*$^{-/-}$*-Phd3*$^{-/-}$*-Hif2a*$^{-/-}$ compared to *Cre*$^{-}$ controls (n=4 for *Foxd1*$^{+/+}$ *Phd2*$^{fl/fl}$ *Phd3*$^{fl/fl}$ *Hif2a*$^{fl/fl}$ control mice; n=3 for *Foxd1-Phd2*$^{-/-}$*-Phd3*$^{-/-}$*-Hif1a*$^{-/-}$ mutants; n=5 each for *Foxd1-Phd2*$^{-/-}$*-Phd3*$^{-/-}$*-Hif2a*$^{-/-}$ mice). Data are represented as mean ± SEM; 2-tailed Student's *t*-test; *p<0.05, **p<0.01 and ***p<0.001. *Acta 2*, α*-smooth muscle actin; Aqp1, aquaporin 1; Aqp2, aquaporin 2; NaPi2a, sodium-phosphate co-transporter-2a; Ncc NaCl co-transporter; Nkcc2, Na-K-2Cl co-transporter Scnn1a, sodium channel epithelial 1 alpha subunit; Trpv5, transient receptor potential cation channel subfamily V member 5.*

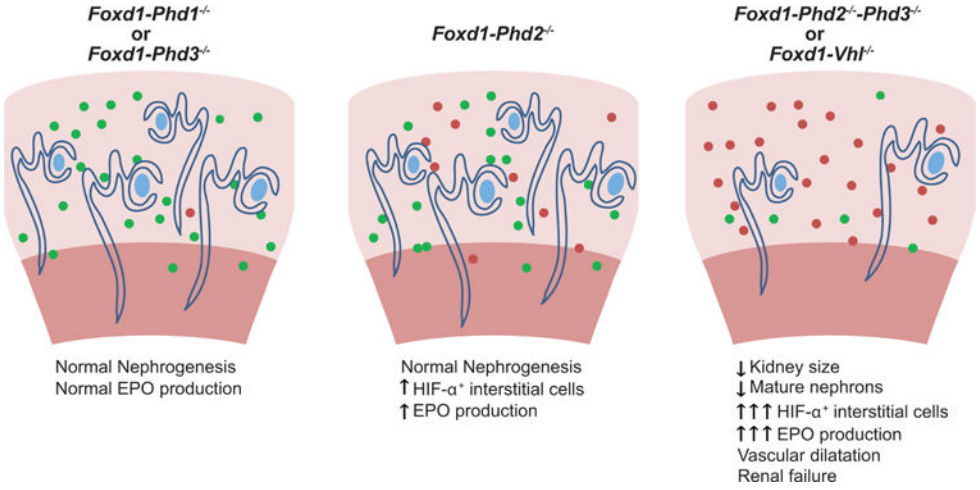

Figure 7. Schematic depicting the role of PHD dioxygenases in renal development

HIF-α^{+} stromal cells are shown as filled red circles, filled green circles depict targeted stromal cells that fail to stabilize HIF-α. Normal EPO production in *Foxd1-Phd1*$^{-/-}$ or *Foxd1-Phd3*$^{-/-}$ mutant mice is indicated by a single filled red circle.